ELSEVIER

Journal of Power Sources 75 (1998) 84–89

JOURNAL OF POWER SOURCES

Investigation of changes in morphology and elemental distribution in metal hydride alloys after electrochemical cycling

Wenlin Zhang [a,*,1], Arnaldo Visintin [a,2], Supramaniam Srinivasan [a,3], A. John Appleby [a], Hong S. Lim [b]

[a] *Center for Electrochemical Systems and Hydrogen Research, Texas Engineering Experiment Station, Texas A&M University System, College Station, TX 77843-3402, USA*

[b] *Hughes Space and Communications, Torrance, CA 90505, USA*

Received 3 February 1998; accepted 1 April 1998

Abstract

Changes in morphology and elemental distributions in a metal hydride alloy particle after electrochemical charge–discharge cycling were studied using scanning electron microscopy and energy dispersive X-ray analysis. Electrochemical performance evaluation of the metal hydride electrodes included capacity degradation, charge–discharge rate capability, and electrode impedance after a varying number of cycles. These were correlated with the morphology and the elemental distribution changes. Results showed that Al migrates toward the surface from the bulk of an alloy particle as the electrode is cycled. At the same time, the electrode impedance due to charge transfer resistance is reduced significantly. The reduction in impedance correlates with an improved rate capability of the electrode on cycling. The presence of Al in the alloys studied appears to improve cycle life.

Keywords: Metal hydride; Batteries; Capacity; Rate capability; Morphology

1. Introduction

Hydrogen storage alloys which reversibly form hydrides during the electrochemical charge/discharge process [1,2] have been used as the anode material in nickel/metal hydride (Ni/MH_x) secondary batteries for consumer electronics during the last decade [3]. The wt.% of hydridic hydrogen determines the maximum capacity (A h/g) of the metal hydride electrode. The overall performance of a metal hydride electrode depends strongly on the structure and composition of the alloy and on the electrode fabrication technique, since the alloy expands when hydrides form during charging. An electrode structure in the form of a flexible three-dimensional network is necessary to provide stable intimate contact between active alloy particles and the current collector. The effects of the composition and structure of metal hydride electrodes on their performance have been investigated [4]. This showed that performance and cycle life of a metal hydride depends on its fabrication history.

The mechanism of the hydriding/dehydriding reaction has been investigated using electrochemical impedance spectroscopy (EIS) [5]. It was found that the rate capability on charge and discharge is determined by the kinetics of the charge transfer reaction at the alloy surface. The rate capability is also strongly influenced by (i) the nature of electrode additives; and (ii) the amount of active material, since these directly affect the contact between the alloy surface and the electrolyte. It is known that the performance of a metal hydride electrode, particularly its discharge capacity, deteriorates on continued charge/discharge cycling. However, the changes of morphology, structure, and composition of the metal hydride alloy with cycling, and their correlation with performance deterioration, are not well understood. The segregation of substituent elements in a hydride electrode has been reported [6]. This is believed to be a contributing factor to the degradation of alloy particles. Studies on elemental segre-

* Corresponding author.

[1] Present address: Schlumberger Perforating and Testing Center, P.O. Box 1590, Rosharon, TX 77583, USA.

[2] Present address: Instituto de Investigaciones Fisicoquímicas Teóricas y Aplicadas (INIFTA), Sucursal 4, Casilla de Correo 16, 1900 La Plata, Argentina.

[3] Present address: Center for Energy and Environmental Studies, Princeton University, Princeton, NJ 08544-5263, USA.

0378-7753/98/$19.00
PII S0378-7753(98)00095-0

Table 1
Electrochemical characteristics of hydride electrodes

Sample	Compositions	Maximum capacity (mAh/g)	Capacity degradation rate (mAh/g/cycle)
H149	$La_{0.7}Ce_{0.3}Ni_{3.55}Al_{0.3}Co_{0.75}Mn_{0.4}$	323	0.22
H153	$La_{0.6}Ce_{0.3}Zr_{0.1}Ni_{3.55}Al_{0.3}Co_{0.75}Mn_{0.4}$	274	0.47
H201	$La_{0.7}Ce_{0.3}Ni_{3.55}Co_{0.75}Mn_{0.7}$	320	0.92

gation in a metal hydride alloy particle after electrochemical charge/discharge cycles have not been previously reported. This is because of the experimental difficulties in analyzing elemental distribution in small alloy particles, since XPS surface analysis is not applicable to three-dimensional porous electrodes containing active hydride alloy powder dispersed in the matrix.

In this work, the morphological and elemental distribution changes in a metal particle were studied as a function of cycle life using scanning electron microscopy and energy dispersive X-ray analysis. The electrochemical performance of the electrode, including capacity degradation, charge/discharge rate capability, and changes in electrochemical impedance, were also studied as a function of cycle life.

2. Experimental

2.1. Fabrication of metal hydride electrodes

Metal hydride (MH_x) test electrodes were prepared by pasting a slurry of the alloy powder, Shawinigan acetylene black (AB50), and polybenzimidazole binder solution on a piece of nickel foam substrate with 80 to 100 pores per linear inch. Test electrodes were approximately 2.3 cm × 2.3 cm in size. Electrodes made by this process contain a high proportion of the active material, typically 80% of the electrode weight excluding tabs [7]. Each electrode contained approximately 0.8–1.0 g of alloy. The composition of hydride-forming alloys used in these electrodes is listed in Table 1. Two sample electrodes were made from each alloy, one for a cycle life test, and another for a short-term cycle test, which was followed by SEM examination for the changes of the alloy particles and electrode structure.

2.2. Cycle life behavior and rate capabilities

The counter electrode was a standard sintered nickel oxide electrode which had a much larger geometric area and capacity than the working electrode. The 31 wt.% KOH electrolyte was prepared from reagent grade KOH

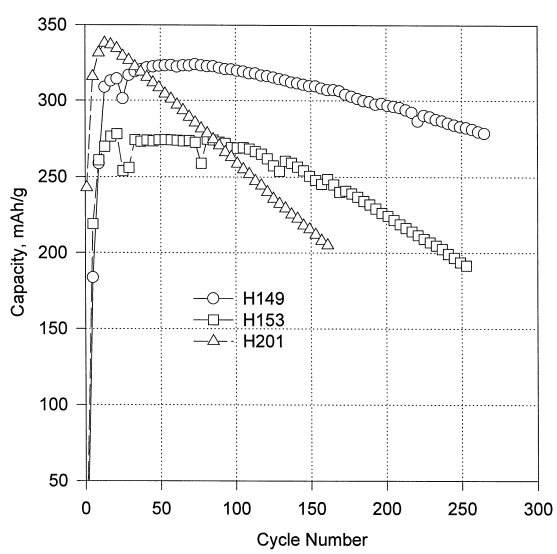

Fig. 1. Change in specific capacity of the metal hydride electrodes H149, H153, and H201 during cycle life test.

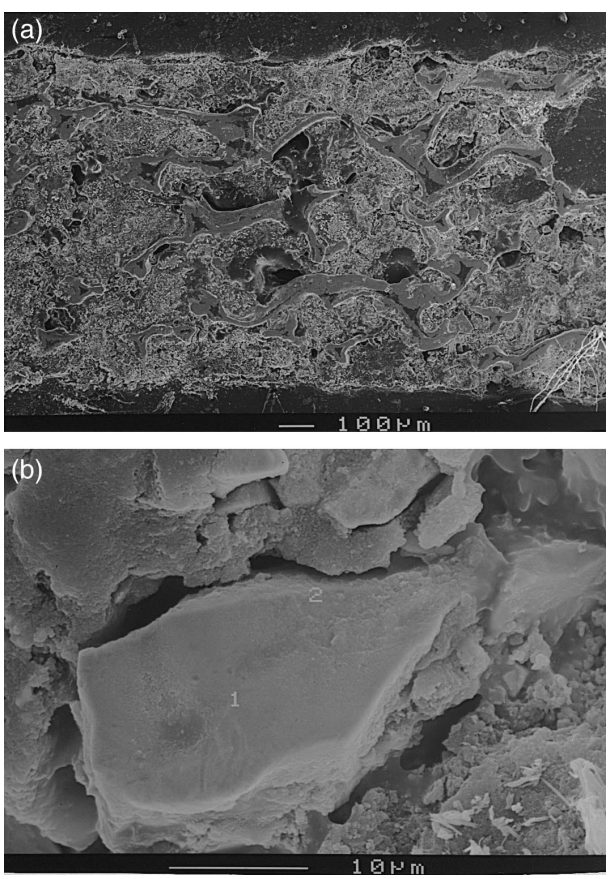

Fig. 2. SEM image of H149 electrode sample after 20 cycles. (a) Electrode structure. (b) Morphology of alloy particles.

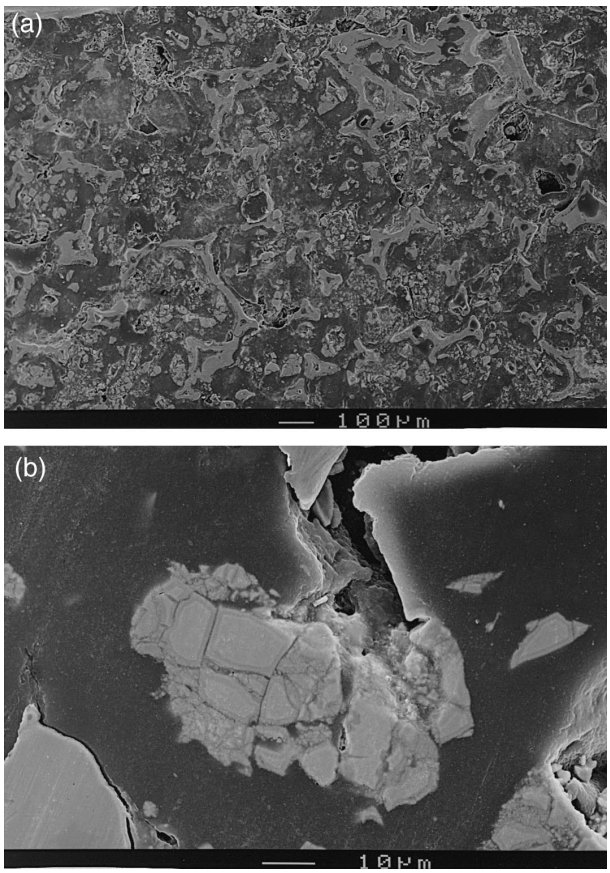

Fig. 3. SEM image of H149 after 270 cycles. (a) Electrode structure. (b) Morphology of alloy particles.

and deionized water. The electrochemical study included measurements of charge/discharge behavior and rate capability of the electrodes at 25°C. The electrochemical measurements were made in a flooded electrolyte condition in open cells. The capacity was measured to a cut-off potential of −0.7 V vs. a Hg/HgO reference electrode. Cycle life and capacity measurements were made using an Arbin Battery Cycler (Arbin Instruments, College Station, TX) by charging at the 0.5 C rate for 2.5 h and discharging at the same rate to the cut-off potential. The charge rate capability was determined by charging the electrodes at different rates, followed by discharge at 0.5 C. The discharge rate capability was similarly obtained by charging at 0.5 C, followed by discharge at various rates to the cut-off voltage.

2.3. Electrochemical impedance spectroscopy studies

The equipment for electrochemical impedance spectroscopy (EIS) consisted of a Princeton Applied Research M273 Potentiostat/Galvanostat and a M3501A Lock-in Amplifier controlled by an IBM PS/2 personal computer. The EIS experiments, at open-circuit potential, were carried out after a desired number of charge/discharge cycles. The impedance data were obtained in the frequency range of 0.001–20,000 Hz. The amplitude of the modulated signal was 5 mV.

2.4. SEM–EDAX studies of metal hydride electrodes

Scanning electron microscopy (SEM) and energy dispersive X-ray (EDX) studies were carried out using a JSM model 6400 scanning electron microscope equipped with a Noran I-2 EDX unit. The tests were carried out on both the cross-section and the surface of the electrode. For the cross-section SEM–EDX examinations, the electrode samples were prepared by potting the electrodes in an Araldite epoxy mixture. The potted electrode cross-section was polished using 0.3 mm alumina powder. The cross-section of the polished electrodes was then coated with a thin film of Au or Pd to increase the electron conductivity to improve SEM imaging.

2.5. Experimental procedures

The electrodes were initially charged and discharged at the 0.5 C rate for about 20 cycles. This was followed by rate capability measurements. Electrochemical impedance measurements were conducted on selected electrode sam-

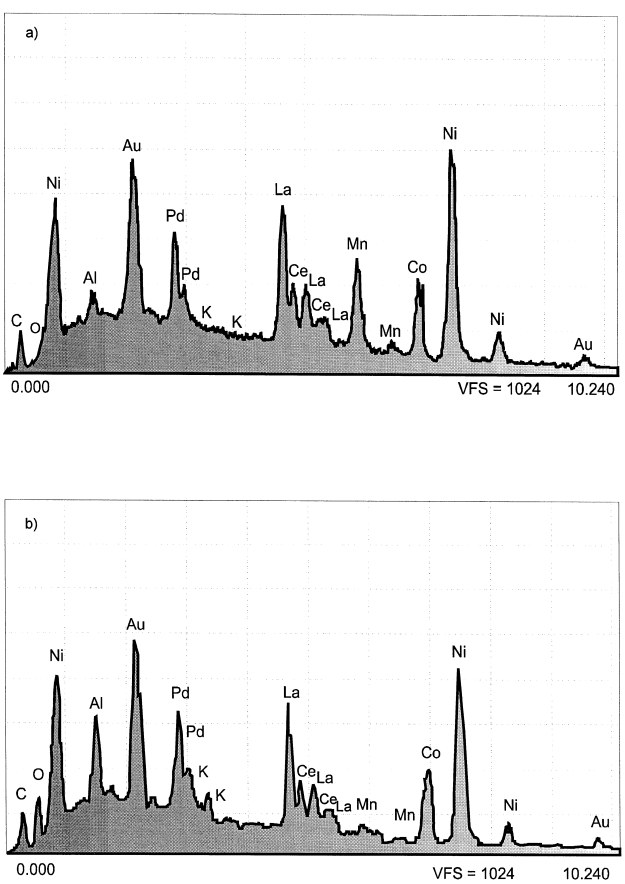

Fig. 4. (a) EDAX elemental analysis results of H149 at the center of an alloy particle after 270 cycles. (b) EDAX analysis results at the particle surface after 270 cycles.

ples and were followed by 100% discharge and preparation for SEM/EDAX examination. Cycling of similar metal hydride electrodes was continued to 270 cycles, the electrodes also being subjected to SEM/EDAX examination. Interim rate capability and EIS measurements were carried out after 70, 170 and 270 cycles.

3. Results

3.1. Electrochemical performance

Specific capacity changes of three hydride alloys, numbers H149, H153, and H201, during electrode cycle life testing at the C/2 rate, are shown in Fig. 1. The maximum electrochemical capacity and the capacity degradation rate are shown in Table 1. The specific capacity of sample H149 reached a maximum value of 323 mAh/g after approximately 50 cycles. The H149 electrode showed good cycle life with a capacity retention of greater than 85% of its maximum capacity after 250 cycles. The maximum specific capacity of the H153 alloy was 274 mAh/g, and it retained about 70% of the maximum capacity after 250 cycles. The H201 alloy became fully activated to a high specific capacity of approximately 320 mAh/g, but it degraded rapidly compared with the two other samples, as Fig. 1 shows. Its specific capacity was reduced to 63% of its maximum value after 150 cycles.

3.2. Morphology, structure, and element distribution

Changes in alloy morphology and in elemental distribution in alloy particles during electrochemical cycling were studied using SEM and energy dispersive X-ray analysis (EDAX). Representative SEM images of a cross-section of the H149 electrode sample after 20 and 270 cycles are shown in Fig. 2a and Fig. 3a, respectively. Pulverized alloy particles are observed in the electrode (Fig. 3a) and a separate Al-rich second phase (Al rich) was also present on the particle surfaces (Fig. 3b, Fig. 2b). Other than further particle pulverization, no significant structural changes were observed after 270 cycles (Fig. 2a, Fig. 3a). EDAX analysis after 20 cycles showed that the elemental distribution across the alloy particles was relatively uniform. After 270 cycles, however, EDAX analysis indicated a significant segregation of Al between the bulk and the alloy particle surfaces (Fig. 4a and b). The bulk composition of the alloy particles did not change significantly. The presence of Al is barely detected in the bulk alloy particles because of its low EDAX sensitivity, but it increased significantly near the particle edges and increased sharply at the surface (Fig. 4a and b). Alloy H201 does not contain Al. Particle pulverization in it was observed by SEM after 270 cycles, but apart from the loss of the Mn peaks, no further elemental redistribution was identified using EDAX.

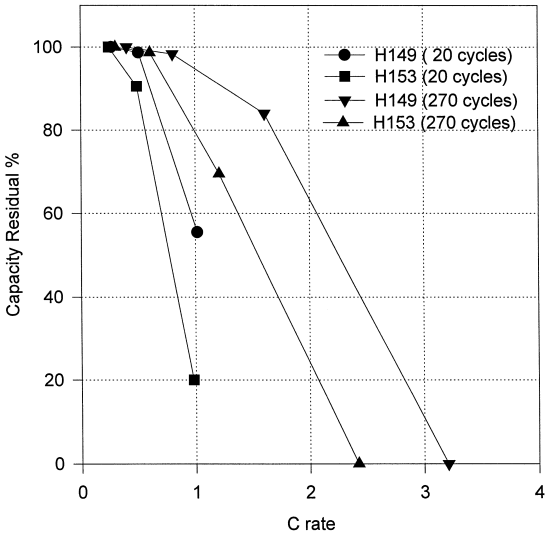

Fig. 5. Rate capabilities of H149 and H153 metal hydride electrode samples.

The loss of Mn may possibly have been due to the low solubility of Mn^{+2} in the electrolyte.

3.3. Charge / discharge rate capabilities and impedance

Measurements of electrode rate capability were carried out after approximately 20 cycles and 270 cycles. For discharge rate capability studies, electrodes were charged at C/2 for 2.5 h to full charge, and then were discharged at C/4, C/2, C, 2 C, and 3 C to a cut-off voltage of −0.7 V vs. Hg/HgO. Fig. 5 shows the discharge rate capabilities for the H149 and H153 electrode samples after 20 and 270 cycles. Their rate capability improved significantly after 270 cycles, as shown by their improved capacity at high rates.

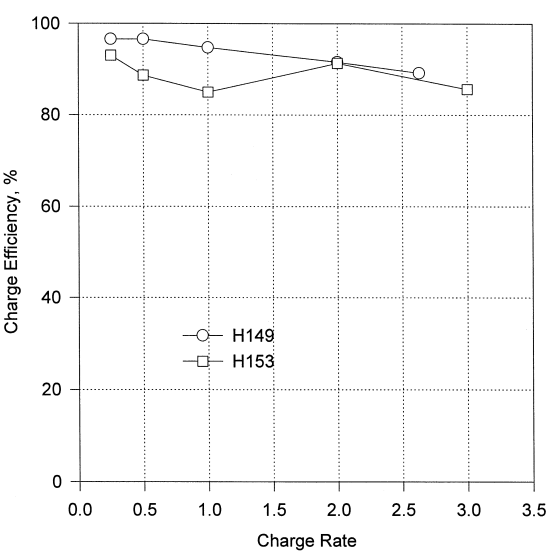

Fig. 6. Charge efficiency of H149 and H153 metal hydride electrode samples.

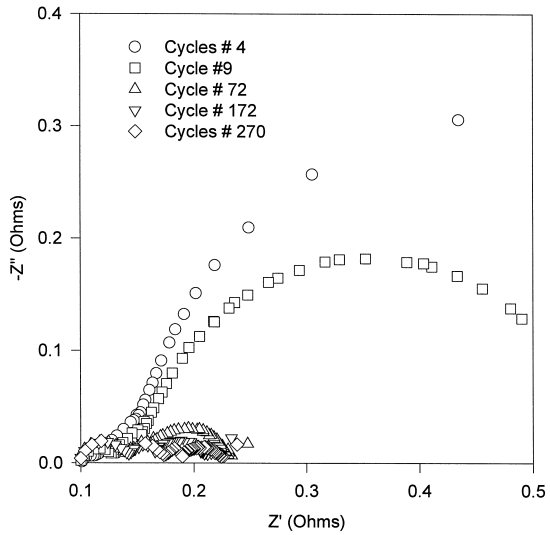

Fig. 7. The Nyquist plots of H149 metal hydride electrode after a varying number of charge/discharge cycles. Electrodes in fully charged state.

For charge efficiency testing, electrodes were charged at C/4, C/2, C, 2 C, and 3 C to full charge as determined by the capacities obtained in previous discharge tests, and then were discharged at the C/2 rate. This was conducted after previously cycling to obtain the completely activated electrode. The charge efficiency is defined as the capacity obtained during discharge as a percentage of the charge capacity. In Fig. 6, the charge efficiency is plotted as a function of charge rate. The charge efficiency was higher than 80% at the 3 C rate for all electrodes. However, it was found that the electrode potential was about −1.4 V vs. Hg/HgO at high rates of charge.

Electrochemical impedance measurements were conducted on the fully charged hydride electrodes under open circuit conditions. Figs. 7 and 8 show typical Nyquist plots

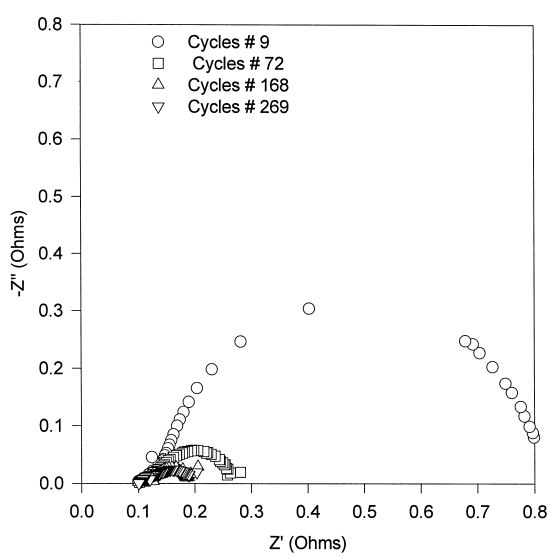

Fig. 8. The Nyquist plots of H153 metal hydride electrode after a varying number of charge/discharge cycles. Electrodes in fully charged state.

for electrodes H149 and H153 after a varying number of charge/discharge cycles. In both cases, the low-frequency semi-circle decreased significantly in size with increasing cycle life, indicating that the resistance of the reaction associated with that semi-circle is reduced by cycling. The resistance stabilized after approximately 170 cycles for both electrodes. This resistance is believed to result from the charge transfer reaction [5]. The reduction of this resistance is apparently related to the improvement in electrode rate capability discussed above.

4. Discussion

The improved cycle life of H149 compared with that of the other alloys appears to be due to the presence of Al as one of the partial substituents of Ni in the B-component of the AB_5 alloy. The presence of Zr as a partial substituent for La in H153 gave reduced capacity and shorter cycle life than a similar alloy (H149) without this substitution. The reduced capacity of the alloy containing Zr (H153) may result from its slightly higher equilibrium plateau pressure than that of the H149 alloy. When the equilibrium plateau pressure approaches atmospheric, part of the hydrogen in the charged hydride alloy may escape to the atmosphere by desorption, thus losing capacity. The reduced rate capability of H153 compared with H149 (Fig. 5) may be due to the high charge transfer resistance of Zr-substituted alloys [5]. The high overpotential for charge rates exceeding 2 C indicates a high kinetic or diffusional resistance in the alloy particles.

The present results indicate that Al atoms migrate from the bulk of the alloy particle toward its surface as the alloy is cycled. One may speculate that accumulation of Al as an insoluble oxide at the surface (possible mix metal oxide-alumina) might serve as a protective film preventing long-term corrosion and extending the alloy's cycle life. Similar protective insoluble film formation by a cerium oxide has been reported for a Ce-containing alloy [8,9]. One may also speculate that insoluble aluminum oxide might serve as an electrocatalyst for the electrode reaction since Al improves the rate capability of the electrode as the cycle life increases (Fig. 5). It may also increase the surface area of the alloy via pulverization [10,11], but this may equally result in poor electrical contact between the pulverized particles.

SEM images (Fig. 2aFig. 3a) show that the compact structure of the electrodes was scarcely changed by cycling. From the equivalent circuit of a metal hydride electrode [5], its interparticle contact properties are determined by its impedance in the high frequency domain of the Nyquist plot. The lower resistance shown in the Nyquist plots for electrodes H149 and H153 may be associated with pulverization and therefore increase surface area and

lower real current density. Thus, the SEM results are consistent with and support the impedance analysis.

5. Summary

It has been demonstrated that Al migrates toward the surface from the bulk of the particle in an Al-containing hydride alloy electrode as cycling proceeds. The rate capability of these hydride electrodes improved with extended charge–discharge cycling. This result is consistent with the EIS results of decreased charge transfer resistance with continued cycling. A partial substitution of the B-component by Al improved alloy performance and cycle life, but a partial substitution of the A-component by Zr caused decreased capacity with no improvement in cycle life.

Acknowledgements

This work was supported by the Chemical Sciences Division, Office of Basic Energy Sciences, U.S. Department of Energy (Contract No. DE-FG03-93ER14381) and the NASA Center for Space Power at Texas A&M University (Contract No. P.O. NAGW-194). The metal hydride alloys H149, H153, and H201 were prepared by J.J. Reilly, J.R. Johnson and G.D. Adzic of the Brookhaven National Laboratory.

References

[1] J.J.G.S.A. Willems, J.R.G.C.M. van Beeks, K.H.J. Buchow, U.S. Patent No. 4,487,817, December 1984.
[2] S.R. Ovshinsky, B. Hills, M.A. Fetcenko, R. Hills, U.S. Patent No. 5,277,999, January 1994.
[3] F.E. Lynch, J. Less-Common Metals 172–174 (1991) 943.
[4] K. Petrov, A. Visintin, S. Srinivasan, A.J. Appleby, Ext. Abs. Electrochem. Soc., Spring Meeting, Electrochemical Society, Pennington, NJ, 1993, p. 41.
[5] W. Zhang, M.P.S. Kumar, S. Srinivasan, H.J. Ploehn, J. Electrochem. Soc. 142 (1995) 2935.
[6] H. Zhang, S. Zhu, Chin. J. Appl. Chem. 9 (2) (1992) 123.
[7] H.S. Lim, G.R. Zelter, J. Power Sources 66 (1997) 97.
[8] M.P.S. Kumar, K. Petrov, W. Zhang, A.A. Rostami, S. Srinivasan, G. Adzic, J.R. Johnson, J.J. Reilly, H.S. Lim, J. Electrochem. Soc. 142 (1995) 3424.
[9] S. Srinivasan, W. Zhang, M.P.S. Kumar, A. Visintin, S. Mukerjee, J. McBreen, G. Adzic, J.R. Johnson, J.J. Reilly, R.B. Schwarz, M.L. Wasz, H.S. Lim, Proc. 11th Annual Battery Conference on Applications and Advances, Long Beach, CA, January 9–12, 1996.
[10] T. Sakai, H. Yoshinaga, H. Miyamura, Kuriyama, J. Alloys Compounds 180 (1992) 37.
[11] H.S. Lim, G.R. Zelter, D.U. Allison, J. Power Sources, in press.